JOURNAL OF DEGRADED AND MINING LANDS MANAGEMENT
Volume 12, Number 2 (January 2025):7095-7109, doi:10.15243/jdmlm.2025.122.7095
ISSN: 2339-076X (p); 2502-2458 (e), www.jdmlm.ub.ac.id

Research Article

Mapping landslide susceptibility in Enfraz to Addis Zemen area Northwestern Ethiopia

Azemeraw Wubalem[1,2*], Belete Getahun[1], Yohannes Hailemariam[3], Alemu Mesele[1], Gashaw Tesfaw[1], Zerihun Dawit[1], Endalkachew Goshe[4]

[1] Department of Geology, College of Natural and Computational Science, University of Gondar, Gondar, Ethiopia
[2] Department of Earth Science, University of Turin, Turin, Italy
[3] Department of Civil Engineering, School of Civil and Hydraulic and Water Resource-Engineering, the Institution of Technology, University of Gondar, Gondar, Ethiopia
[4] Department of Hydraulic and Water Resource Engineering, School of Civil and Hydraulic and Water Resource-Engineering, the Institution of Technology, University of Gondar, Gondar, Ethiopia

[*]corresponding author: alubelw@gmail.com

Article history:
Received 13 September 2024
Revised 21 October 2024
Accepted 5 November 2024

Keywords:
Ethiopia
frequency ratio
GIS
landslides
susceptibility

Abstract

The study area (Enfraz to Addis Zemen) is located in northwestern Ethiopia, which frequently experiences landslides, causing damage to farmland, engineering structures, infrastructures, and villages, as well as animal and human fatalities. To manage this catastrophic hazard, a comprehensive GIS-based frequency ratio model (FR) was applied to produce a landslide susceptibility map. In this study, 134 landslides were identified from detailed fieldwork and Google Earth imagery analysis, split into 70% to develop the model and 30% for model validation. The relationship between landslide probability with landslide factor classes of lithology, annual mean rainfall, slope, aspect, curvature, elevation, distance to the river, and land use-land cover was analyzed in a GIS environment. FR model assigns weights to each factor class based on observed frequencies. These weighted factors were summed using a raster calculator to produce landslide susceptibility indexes (LSIs), which were classified into very low, low, moderate, high, and very high susceptibility classes using the natural break classification method. The model's accuracy and performance were validated using the area under the curve of the receiver operating characteristics curve (ROC), which showed an AUC success rate of 92.2% and a predictive rate of 86.05%. These results confirm that the FR model is effective in landslide susceptibility modeling. The generated map can support decision-makers, urban planners, and researchers in land use planning, landslide mitigation strategies, and future research.

To cite this article: Wubalem, A., Getahun, B., Hailemariam, Y., Mesele, A. Tesfaw, G., Dawit, Z. and Goshe, E. 2025. Mapping landslide susceptibility in Enfraz to Addis Zemen area Northwestern Ethiopia. Journal of Degraded and Mining Lands Management 12(2):7095-7109, doi:10.15243/jdmlm.2025.122.7095.

Introduction

Landslides become dangerous geological hazards and occur when gravitational forces exceed the resisting forces in the slope, causing the downslope or upward movement of earth materials (Wubalem and Meten, 2020; Wubalem et al., 2022; Liu et al., 2024). Landslide events have caused fatality, environmental degradation, and damage to infrastructure, eventually obstructing sustainable development (Fang et al., 2021; Zhu et al., 2023; Liu et al., 2024). Globally, landslide occurrence and magnitude continuously increase as anthropogenic disturbance, climate change, and earthquake events increase (Gautam et al., 2021; Wubalem et al., 2022; Putriani et al., 2023). Mapping and understanding landslides are very important to

land use planning and prevention strategies (Wubalem et al., 2022; Liu et al., 2024).

In the highland part of Ethiopia, particularly in southern, central, and northern areas as well as along the main Ethiopian rift valley margins, landslide incidences frequently occur (Wubalem et al., 2022). These phenomena are mainly triggered by heavy and prolonged rainfall, improper land practice, and earthquakes in the rift margin, causing human and animal fatality, wide-ranging damage to engineering structures, villages, infrastructure, and property as well as destruction of farmlands and environments (Mersha and Meten, 2020; Wubalem and Meten, 2020; Getachew and Meten, 2021; Wubalem et al., 2022; Mulugeta et al., 2024).

The most recent landslide incident confirms the frequent occurrence and its level of impact in Ethiopia. For example, on July 22, 2024, highly intensified rainfall for a long time in regions with preconditions of steep terrain and unconsolidated soil layers resulted in a large debris flow in Kencho Shacha Gozdi Kebele, Gofa Zone, Southern Ethiopia, causing over 257 human fatalities. This was followed by another landslide on August 5, 2024, in Tipa Kebele, Khao Koisha District, Walayita Zone, which caused 11 human fatalities. Most recently, on August 23, 2024, a landslide in Abna Kebele, North Gondar Zone, killed 23 people and 35 domestic animals and seriously injured 8 people.

Although landslides reoccur and result in significant damage and fatality, detailed landslide susceptibility modeling is not conducted in different vulnerable parts of the country, including the study area (Enfraz to Addis Zemen area). The study area is an economic corridor that is frequently affected by landslides. A debris flow in 2021 in the study area is a typical example that destroyed agricultural lands, villages, and roads, as well as three human fatalities.

Detailed landslide inventories and susceptibility mapping are critical for effective landslide risk mitigation (Shano et al., 2020; Xiao et al., 2021; Bao et al., 2022; Zhu et al., 2023). Landslide inventories and susceptibility models show the spatial distribution of past landslides and landslide-prone areas, respectively. These maps provide essential information for decision-makers, planners, and engineers in disaster risk reduction and proper land-use practice. High susceptibility risk areas can identified by understanding the processes and the relationship between past landslides and factors that contribute to landslides (Shano et al., 2020; Fang et al., 2021; Bao et al., 2022).

Advancements in technology, such as computers, Geographic Information Systems (GIS), remote sensing, various codes, and processing software, have resulted in the development of many landslide susceptibility modeling techniques ranging from expert-driven qualitative, semi-quantitative (e.g., Analytical Hierarchy Process) to advanced data-driven quantitative techniques (e.g., Statistical, machine learning). Expert-driven methods depend on expert judgment more than data-driven approaches. Despite the fact that machine learning approaches provide high-accuracy results, they often require substantial computational resources (Wubalem et al., 2022), while statistical methods (e.g., the bivariate Frequency Ratio (FR)) are routinely used because of their simplicity, efficiency, and reliability in landslide susceptibility mapping (Nachappa et al., 2020; Gautam et al., 2021; Putriani et al., 2023).

Although the study area experienced frequent reoccurrence of landslides, no previous research has been conducted to assess the region's susceptibility. This study aimed to develop a comprehensive landslide susceptibility map for the Enfraz to Addis Zemen road section using the Frequency Ratio (FR) method. The relationship between past landslides and landslide factor classes of slope, lithology, elevation, annual mean rainfall, aspect, curvature, distance to rivers, and land use was quantified using the FR model. Detailed fieldwork, Google Earth imagery, GIS, and FR statistical methods were applied. The landslide susceptibility model can provide an essential tool for decision-makers, planners, and engineers in long-term land-use planning, infrastructure development, and disaster risk management. This research may reduce the socio-economic and environmental impacts of landslides in the region and inspire researchers to further research in other parts of Ethiopia.

Materials and Methods

Study area and geological setting

The Enfraz to Addis Zemen road (study area) is located in the Northwestern highlands of Ethiopia (Figure 1) and lies within a landslide-prone region. This area is characterized by various landscape features, including a plateau, deep gorges, and rugged topography with elevation ranges from 1,843 m to 3,014 m above sea level (Figure 3). The area has a bimodal rainfall pattern, with a high precipitation from July to September. During this period, the area receives high amounts and prolonged rainfall, causing saturation of soils and increasing the probability of landslides. The month from November to June is characterized by minimal rainfall. The mean annual rainfall in the area is maximum and minimum values of 112.2 mm and 98 mm (Figure 3d), respectively.

Data source

Table 1 presents key data sources and their respective details. Various data were gathered from primary and secondary data sources. The landslide inventory data were obtained from detailed fieldwork and Google Earth imagery analysis. The Digital Elevation Model (DEM) with a spatial resolution of 12.5 m was downloaded from NASA's Earth Data platform. Topographic parameters such as aspect, curvature, slope angle, and elevation as well as distance to

drainage, were prepared from DEM. The Institute of Ethiopian Geological Survey (IEGS) provided regional geological data, including lithology and lineament information.

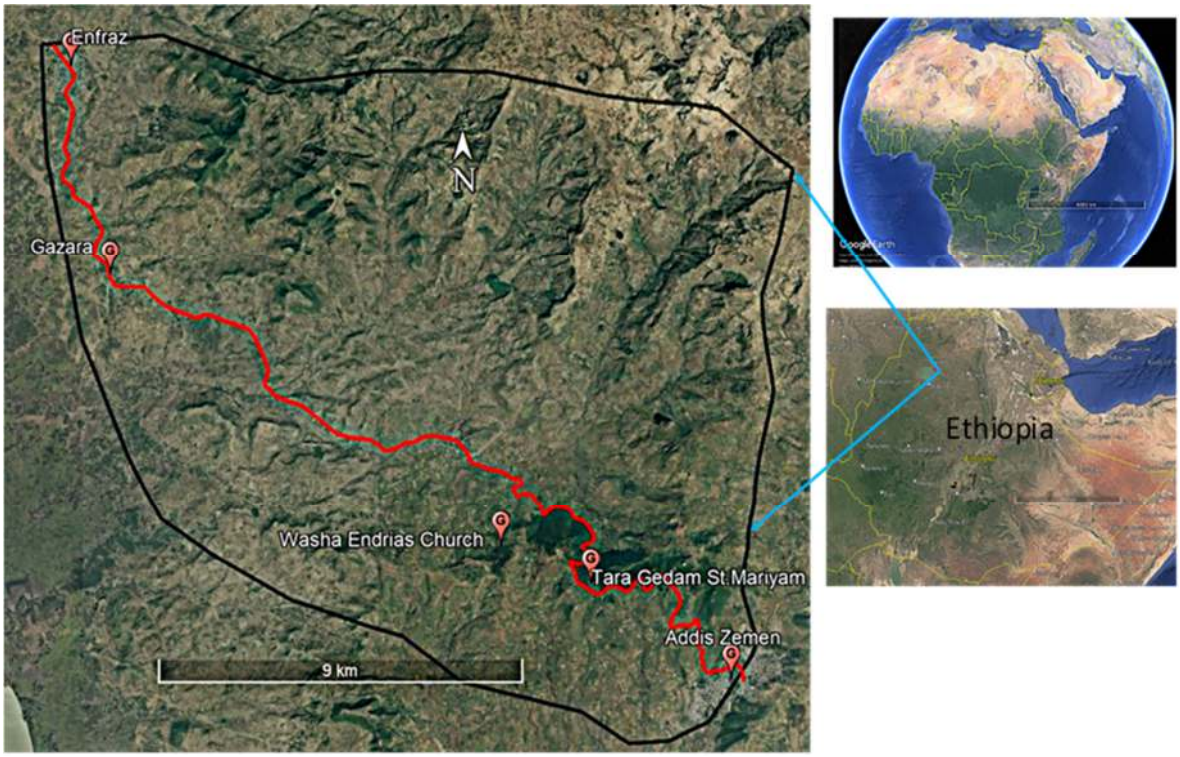

Figure 1. Location map of the study area.

Table 1. Data source and data type.

Data type	Spatial resolution	Variable	Sources
DEM	12.5 m	Slope angle, aspect, curvature, distance to drainage, and elevation map	NASA earth data (https://search.asf.alaska.edu)
Geological map	1:250,000	Lithology and lineaments	Institute of Ethiopian Geological Survey (IEGS)
Google Earth image		Landslide inventory	NASA/Google Earth
Rainfall (1989-2019 years)	---	Annual and monthly mean rainfall	Ethiopian National Meteorological Agency (NMA)

Rainfall data covering the period from 1989 to 2019 with annual and monthly mean values were collected from the Ethiopian National Meteorological Agency (NMA).

Landslide Inventory

Understanding and mapping the landslide inventory is a crucial first step to understanding landslides spatial-temporal distribution and their consequences. In this work, integrated methods, including detailed fieldwork and Google Earth imagery, were applied to develop a landslide inventory map (Martinello et al., 2021). 134 past landslides were identified and digitized into polygons (Figure 2). The landslide was split into two datasets, 70% training, and 30% testing, guaranteeing their spatial distribution using the subset tool in ArcGIS (Zhang et al., 2022). The total area affected by landslides is approximately 491,038.2 m², with size from 296.5 m² to 29,233.3 m². The study area's landslides are highly concentrated on lineaments, river initiation zones, steep slopes, and weak rock units covered by thin soil layers. The dominant landslide types identified include transitional slides, debris flows, and rockfalls, which reflect the complex interaction of geomorphological, hydrological, and geological factors that influence slope instability.

Landslide conditioning and triggering factors

Assessing factors that are conditioning and triggering landslides is valuable for effective landslide risk mitigation (Wubalem et al., 2022). According to the literature, major contributors to landslide susceptibility globally include anthropogenic activities, topography,

geology, hydrology, and seismic events. The interaction of these factors influences landslide frequency and intensity in specific regions (Gautam et al., 2021; Li et al., 2022; Putriani et al., 2023). For the study area, eight key factors were selected based on the geo-environmental conditions, data availability, and landslide inventory data (Nachappa et al., 2020; Zhu et al., 2023). These factors include slope degree, aspect, curvature, distance/proximity to river, elevation, lithology, mean annual rainfall, and land use-land cover. To evaluate their variability and impact on landslide susceptibility, these factors were classified into subcategories using the natural break classification method.

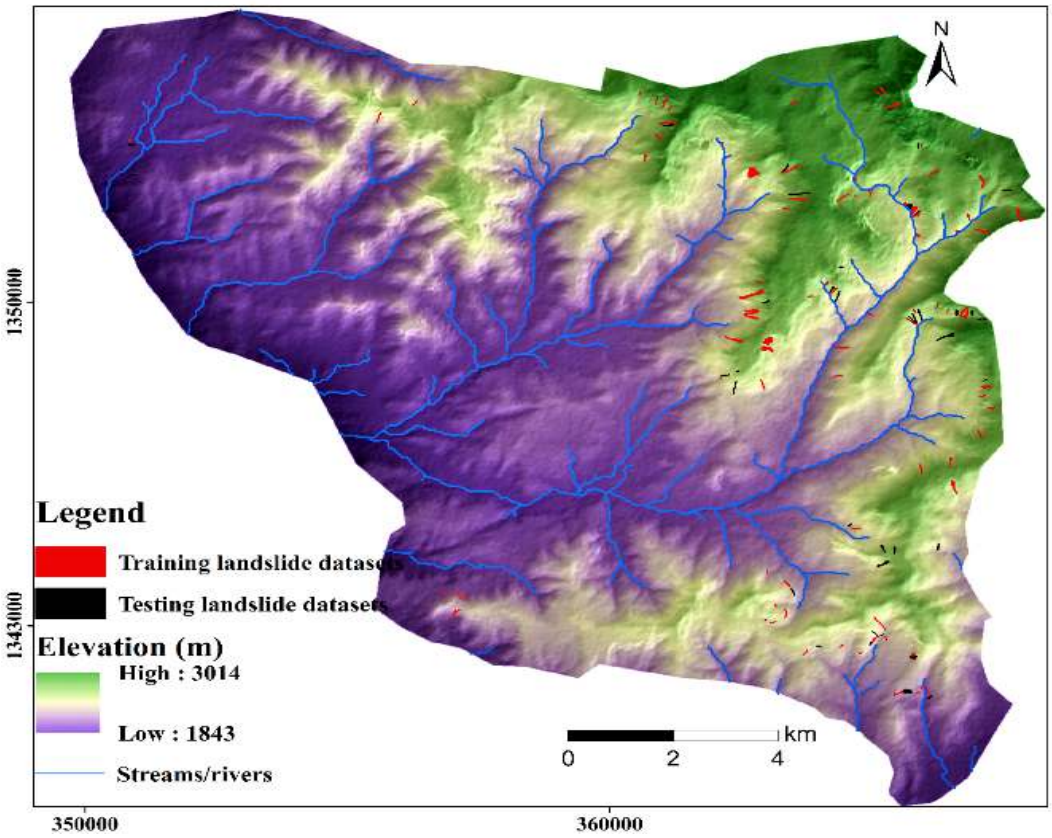

Figure 2. Landslide inventory map of the study area: red polygons are training landslide datasets, and black polygons are testing landslide datasets.

Geological factors

Geological factors, including lithology and geological structures/lineaments, play a great role in landslide occurrences, controlling the type and size of landslides (Nachappa et al., 2020; Roccati et al., 2021; Wubalem et al., 2022). In this study, only lithology was considered, and it was digitized from a 1: 250,000 scale geological map and updated from fieldwork. The lithology was categorized into highly weathered basalt, moderately weathered basalt, and unconsolidated sediment (Figure 3d).

Topographic factors

In literature, topographic factors such as slope, aspect, curvature, and elevation are commonly used in landslide susceptibility modeling. Slope angle controls stress distribution, surface runoff, and weathered layer depth (Nachappa et al., 2020; Bao et al., 2022; Thanh et al., 2022; Wubalem et al., 2022). The slope map was generated from 12.5-m resolution DEM and was classified into five subclasses (Figure 4f). Furthermore, landslide likelihood controls by the slope aspect depend on solar radiation exposure, wind, rainfall, and other related factors (Nachappa et al., 2020; Roccati et al., 2021; Bao et al., 2022). The aspect was classified into subclasses using natural classification (Figure 4h). The effects of curvature on landslide probability depend on surface and subsurface hydrology, and gravity. The curvature of the study area is classified into three general curvatures: convex, concave, and flat (Figure 3a). Elevation affect rainfall patterns, topography, geology, and human activity (Nachappa et al., 2020). The effects of elevation on landslide likelihood depend on slope gradient, rainfall distribution, soil thickness, vegetation cover, and human activities (Fang et al., 2021). In this study, elevation is classified into six subclasses (Figure 3b).

Hydrological factors

Among hydrological factors, drainage densities and distance to the river are commonly used in landslide

susceptibility modeling. They control sediment deposition, soil moisture, and slope toe erosion (Nachappa et al., 2020; Wubalem et al., 2022). In this study, only distance-to-river was considered and was prepared using Euclidean distance. It was classified into six classes (Figure 3c).

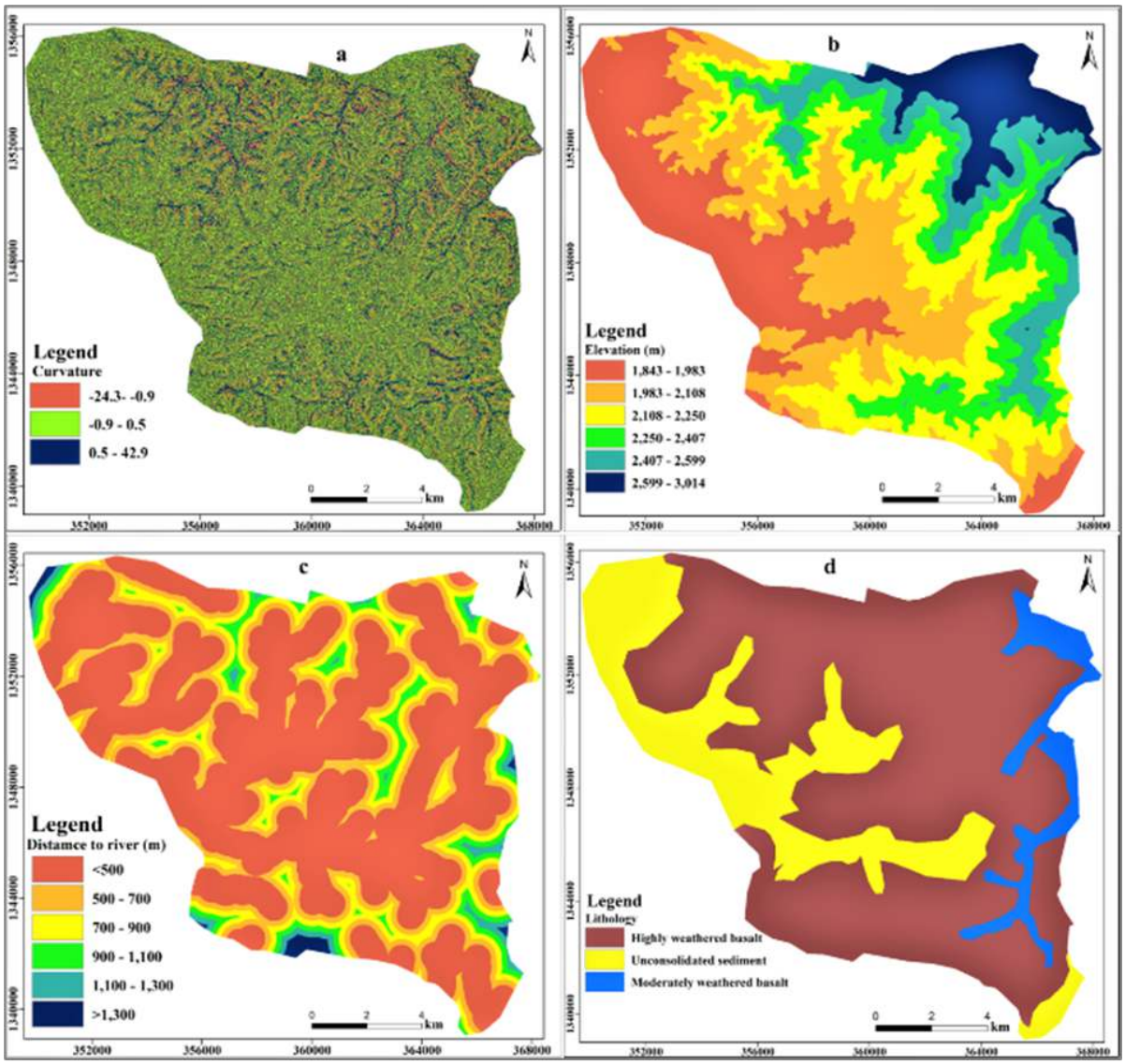

Figure 2. Landslide factor maps of the Enfraz to Addis Zemen: (a) curvature, (b) elevation, (c) distance to river, and (d) lithology.

Land use and climatic Factors

Rainfall is a commonly used landslide-triggering factor in susceptibility modeling. It increases landslide probability through soil saturation and pore water pressure (Nachappa et al., 2020). The annual mean rainfall of the study area was classified into subclasses (Figure 3j). Land use and land cover (LULC) are other landslide factors that influence landslide occurrences but depend on human activities such as urbanization, agriculture, and deforestation. LULC is classified into seven distinct subclasses (Figure 4e).

Research design

In this study, four geodatabases were created to manage the data analysis process: one for landslide factors, two for landslide inventory layer such as training and testing datasets, and one for landslide susceptibility model. Before data processes, all data were standardized with a spatial resolution of 12.5 m and converted to raster format. Furthermore, all parameters were projected to the same coordinate system, Adindan UTM Zone 37N, to ensure correct spatial alignment. A combined tool in the spatial analysis environment of GIS was used to determine the relationship between landslide factor classes and 70% of training datasets. Then the FR model was then applied to assign weights for each class. After weighting the factor classes, they were transformed into raster format based on their FR value using the lookup tool. Eventually, landslide susceptibility indexes (LSIs) were produced. The LSIs were

classified into very low, low, moderate, high, and very high susceptibility classes using the natural break classification method. The model's performance and accuracy were evaluated using the Area Under the Curve (AUC) of the Receiver Operating Characteristic (ROC) curve.

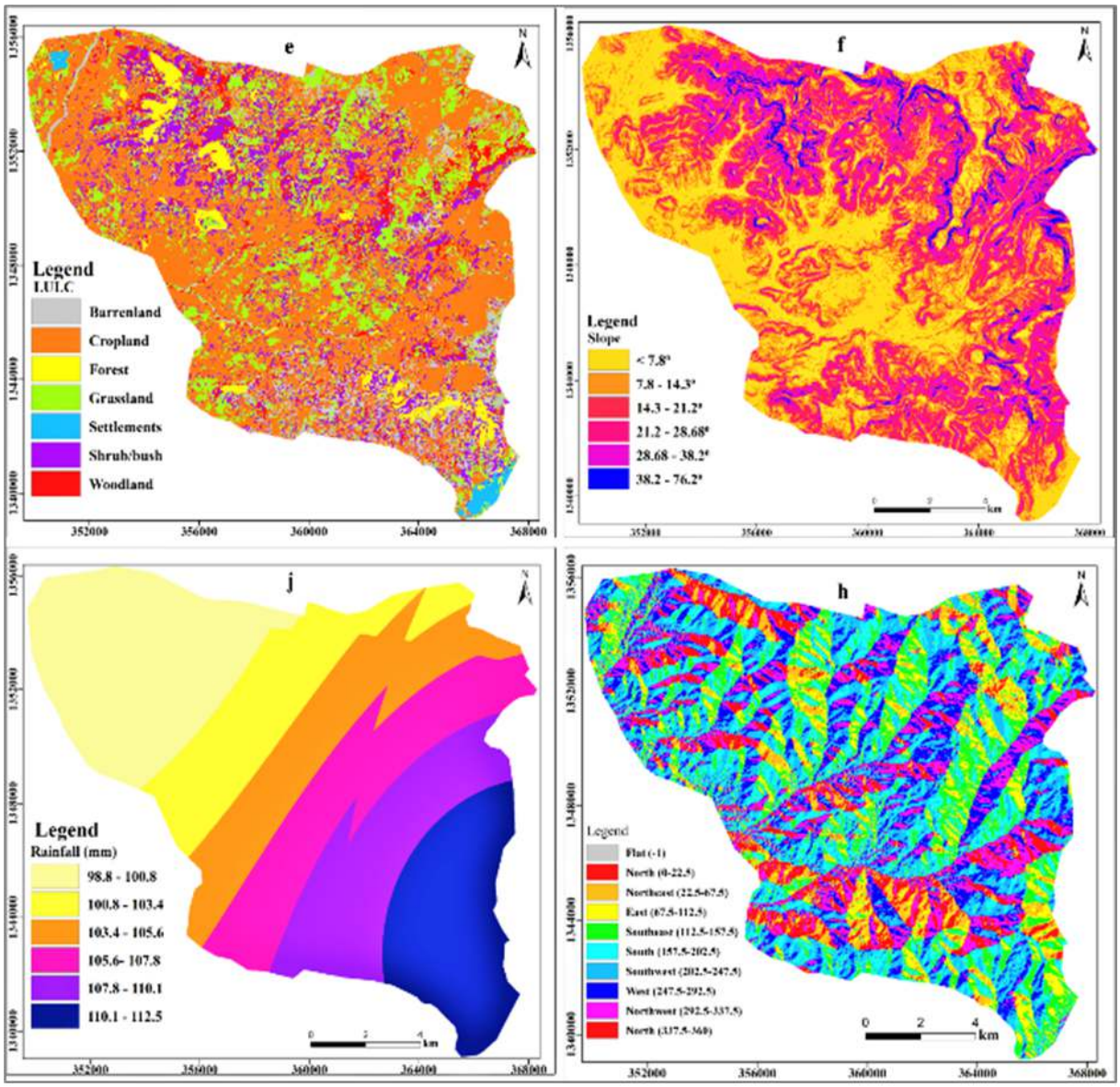

Figure 3. Landslide factor maps of the Enfraz to Addis Zemen: (e) LULC, (f) slope, (j) annual mean rainfall, and (h) aspect.

The training and testing landslide datasets were combined with LSIs. The ROC curve plotted from observed landslides on the y-axis and predicted landslides on the x-axis. AUC values for success and predictive rates were then calculated.

Approaches

Frequency Ratio (FR)

The Frequency Ratio (FR) method is widely recognized for its simplicity, rapid calculation, and reliable results (Nachappa et al., 2020; Gautam et al., 2021; Wubalem et al., 2022; Putriani et al., 2023). This method establishes the relationship between landslides and various landslide factor classes by calculating the FR value, which represents the ratio of the area affected by landslides within a particular factor class to the total area of that factor class. Regardless of its merits, the FR model has shortcomings, such as needing historical landslides and focusing on factor classes. FR values can be calculated using Eq 1. FR value equal to one indicates an average probability. FR>1 indicates a high probability, and FR < 1 indicates a lower probability (Putriani et al., 2023).

$$FR = \frac{S}{Y} = \frac{\frac{Nlspix}{Ntlspix} * 100}{\frac{Ncpix}{Ntcpix} * 100} \quad \text{Eq. 1}$$

The LSIs of this study were generated by summing up all weighted raster factors using Eq. 2.

$$LSI = \sum_{i=1}^{n} FR_i y_i \quad \text{Eq. 2}$$

Where:

- FR is frequency ratio
- Nlspix is the number of landslide pixels within a factor class
- Ntlspix is the total landslide area

Model validation

Landslide susceptibility modeling without validation is not practical. Validation is important to evaluate how the model correctly classifies the region as landslide and non-landslide-prone zones and effectively predicts future landslide probability (Nachappa et al., 2020; Wubalem, 2021). The area under the curve (AUC) of the receiver operating characteristic (ROC) curve is a commonly used technique in model validation (Mersha and Meten, 2020; Wubalem and Meten, 2020; Getachew and Meten, 2021; Putriani et al., 2023; Wubalem et al., 2022).

In this study, the FR model was validated using the AUC of the ROC. For this, landslide datasets were split into 70% training and 30% testing datasets. Then, the LSI was combined with these datasets to perform spatial analysis of the GIS environment. Then, the true positive (TPR), false positive rate(FPR), and AUC were calculated using real statistics extension in Excel. The ROC curve is plotted with the true positive rate on the y-axis and the false positive rate on the x-axis. ROC is useful for graphically assessing a model with a curve closer to the top left corner indicating model classified areas and predicting future probability correctly, but a curve near the diagonal and below the diagonal shows random modeling. The AUC value ranges from 0.5 to 1, with a higher AUC showing high performance and accuracy (Nachappa et al., 2020; Wubalem et al., 2022; Kohno and Higuchi, 2023; Zhu et al., 2023).

Results

The spatial relationship between landslide factor classes and occurrences was analyzed using the Frequency Ratio (FR) method within a GIS environment, and the results are presented in Tables 2 and 3.

Relationship between factor classes and landslide probability

Table 2 and Figure 9 present the FR values for eight-factor classes, calculated using the FR model. The result revealed the relationship between landslide factor classes and landslide probability.

As stated in the literature (Berhane et al., 2023), slope angle is a critical factor for landslide probability. The result shows the FR value increases as the slope gradient increases. The steepest slope class range from 38.4°-76.2° is the most prone to landslides, with A high FR value of 8.09 (Figure 9). This result aligns with theoretical concepts: as the slope gradient increases, the gravitational force increases, causing a higher probability of failure (Hang et al., 2021). The moderate slope classes 28.7°-38.2° and 21.2°-28.7° display large FR values of 3.54 and 1.35, respectively, indicating that moderately steep slopes are also highly susceptible to landslides. These findings emphasize the role of slope gradient in landslide occurrence.

Landslide incidences can be controlled by the aspect or the slope's orientation. In this study, landslide density is higher on southwest-facing slopes (FR = 1.86), followed by south-facing slopes (FR = 1.28) and west-facing slopes (FR = 1.15). These slope faces are characterized by thin soil layers, steep slopes, weathered rock, and barren land.

The elevation class of 2,407-2,599 m has the highest FR value of 4.08, indicating that areas within this elevation range are particularly prone to landslides. This is followed by the 2,250-2,407-m class (FR = 1.84) and the 2,599-3,014-m class (FR = 1.68). The higher susceptibility of these elevation ranges can be related to factors such as greater precipitation, low vegetation cover, and human activities.

Curvature reflects the concavity or convexity of the terrain, influencing water accumulation, flow, and gravitation force distribution. The class -24.3- -0.9, representing concave slopes, has the highest FR value of 1.29, indicating that such areas are more likely to experience landslides. Concave slopes accumulate water, increasing pore pressure in the soil, which can trigger landslides. The curvature class 0.5-42.9 (FR = 1.01) also shows a slight increase in landslide probability, but the effect is less than the concave slope shape.

As stated in the literature (Nachappa et al., 2020; Roccati et al., 2021; Wubalem et al., 2022; Yu et al., 2024), distance to rivers is another significant factor in landslide probability. The FR result shows that distances 900-1,100 m from rivers have the highest landslide probability, with an FR of 2.00. The 500-700 m and 700-900 m classes also show elevated FR values of 1.55 and 1.29, respectively. This suggests that areas at intermediate distances from rivers are more susceptible to landslides, possibly due to the influence of riverbank erosion or saturation of soils near rivers. However, areas closer than 500 m to rivers have a lower FR (0.74), which may indicate that these zones benefit from riverbank stabilization or less intense weathering.

Rainfall is a well-known triggering factor for landslides, and the FR results confirm its impact. The rainfall class 105.6-107.8 mm/year shows the highest susceptibility with an FR of 2.84, indicating that moderate to high rainfall levels show a good relationship with landslide probability. This is followed by the 103.4-105.6 mm/year class

(FR = 1.29) and the 110.1-112.5 mm/year class (FR = 1.06). High rainfall can lead to soil saturation, increasing the likelihood of landslides, particularly in areas with pre-existing vulnerabilities.

Lithology, or the type of rock or soil in an area, significantly affects landslide susceptibility (Yu et al., 2024). The FR analysis shows that moderately weathered basalt has the highest FR value of 3.4, indicating that this rock type is particularly prone to landslides. Highly weathered basalt also shows elevated susceptibility, with an FR of 1.11. These findings suggest that weathered rock materials, which are typically more fractured and less cohesive, are more likely to fail under stress (Hang et al., 2021). In contrast, unconsolidated sediments have a very low FR of 0.02, indicating a much lower likelihood of landslides in these areas because the unconsolidated soil is found in the flat part of the area.

Table 1. FR result summary for Enfraz to Addis Zemen area.

Factors	Class	Class Pixel	% CA	TRLSP	%TRLSP	FR
Lithology	Highly weathered basalt	882673	70.27	1763	78.22	1.11
	Un consolidated sediment	295193	23.50	13	0.58	0.02
	Moderately weathered basalt	78234	6.23	478	21.21	3.40
Rainfall (mm)	98.8-100.8	293336	23.36	44	1.95	0.08
	100.8-103.4	181984	14.49	129	5.72	0.39
	103.4-105.6	194202	15.46	450	19.94	1.29
	105.6-107.8	203265	16.19	1036	45.90	2.84
	107.8-110.1	186850	14.88	224	9.92	0.67
	110.1-112.5	196156	15.62	374	16.57	1.06
Elevation (m)	1843-1,983	266417	21.21	13	0.58	0.03
	1,983-2,108	290296	23.12	80	3.54	0.15
	2,108-2,250	258438	20.58	174	7.70	0.37
	2,250-2,407	189654	15.10	627	27.76	1.84
	2,407-2,599	140575	11.19	1032	45.68	4.08
	2,599-3,014	110420	8.79	333	14.74	1.68
Distance to river (m)	<500	789219	62.85	1050	46.52	0.74
	500-700	227946	18.15	637	28.22	1.55
	700-900	147262	11.73	342	15.15	1.29
	900-1,100	61724	4.92	222	9.84	2.00
	1,100-1,300	20385	1.62	6	0.27	0.16
	>1,300	9257	0.74	0	0	0
Aspect (°)	Flat (-1)	94896	7.59	92	4.08	0.54
	North (0-22.5)	73083	5.84	64	2.84	0.49
	Northeast (22.5-67.5)	106732	8.53	164	7.27	0.85
	East (67.5-112.5)	158670	12.68	229	10.16	0.80
	Southeast (112.5-157.5)	182938	14.62	230	10.20	0.70
	South (157.5-202.5)	200663	16.04	463	20.53	1.28
	Southwest (202.5-247.5)	174129	13.92	584	25.90	1.86
	West (247.5-292.5)	144226	11.53	298	13.22	1.15
	North (337.5-360)	115654	9.24	131	5.81	0.63
LULC	Forest	12157	5.58	133	5.91	1.06
	Woodland	14845	6.81	523	23.23	3.41
	Shrub/bush	32307	14.82	364	16.17	1.09
	Cropland	107856	49.47	645	28.65	0.58
	Grassland	35937	16.48	369	16.39	0.99
	Barren land	13088	6.00	216	9.60	1.60
	Settlements	1848	0.85	1	0.04	0.05
Curvature	-24.3- -0.9	480991	38.30	1114	49.31	1.29
	-0.9-0.5	525842	41.87	692	30.63	0.73
	0.5-42.9	248967	19.83	453	20.05	1.01
Slope	<7.8°	333445	26.65	45	2.00	0.07
	7.8-14.3°	313458	25.06	116	5.14	0.21
	14.3-21.2°	247508	19.78	289	12.82	0.65
	21.2-28.7°	196130	15.68	476	21.11	1.35
	28.7-38.2°	123145	9.84	785	34.81	3.54
	38.2-76.2°	37305	2.98	544	24.12	8.09

Note: CA is the percent of the class area, and TRLP is training landslide pixels.

Land use and land cover also play a crucial role in landslide susceptibility. The woodland class has the highest FR value of 3.41, indicating that areas covered by woodland are particularly susceptible to landslides. This could be due to the steep slopes and scattered vegetation.

Barren land also shows a high landslide probability with an FR of 1.6 due to a lack of vegetation and root systems that can stabilize soil and prevent erosion. Both shrub/bush areas (FR = 1.09) and forests (FR = 1.06) also show marginal susceptibility, while croplands (FR = 0.58) have a much lower landslide probability, possibly due to many of the agricultural activity performed in the low-lying area.

Landslide susceptibility

Table 3 shows that the Landslide Susceptibility Index (LSIs) values for the study area range from 1.9 to 24.1, representing different susceptibility levels. These LSIs values were classified into five categories: very low, low, moderate, high, and very high susceptibility using the natural break classification method (Figure 5). As the LSIs value increases, the area's susceptibility to landslides also increases. Most of the study area falls into the LSI ranges of 5.1-7.5 (34.50%) and 1.9-5.1 (31.60%), indicating that a large portion of the region is classified as having low to moderate susceptibility (Figure 6). The highest susceptibility class (14.3-24.1) comprises only 3.74% of the total area (Thanh et al., 2022).

Table 2. Model summary for Enfraz to Addis Zemen area.

LSI	LSP	% LSP	TRLSP	% TRLSP	LD	TLSP	% TLSP	LDt
Very low (1.9-5.1)	390096	31.60138	16	0.713967	0.022593	32	4.432133	0.140251
Low (5.1-7.5)	425888	34.50087	204	9.103079	0.263851	107	14.81994	0.429553
Moderate (7.5-10.3)	245666	19.90122	461	20.57117	1.033664	134	18.55956	0.932584
High (10.3-14.3)	126617	10.25715	771	34.40428	3.354177	228	31.57895	3.078726
Very high (14.3-24.1)	46160	3.739387	789	35.2075	9.415313	221	30.60942	8.185679

Note: LSI is landslide susceptibility index, LSP is landslide susceptibility pixels, TRLSP is training landslide susceptibility pixels, LD is training landslide density, LDt is testing landslide density, and TLSP is testing landslide susceptibility pixels.

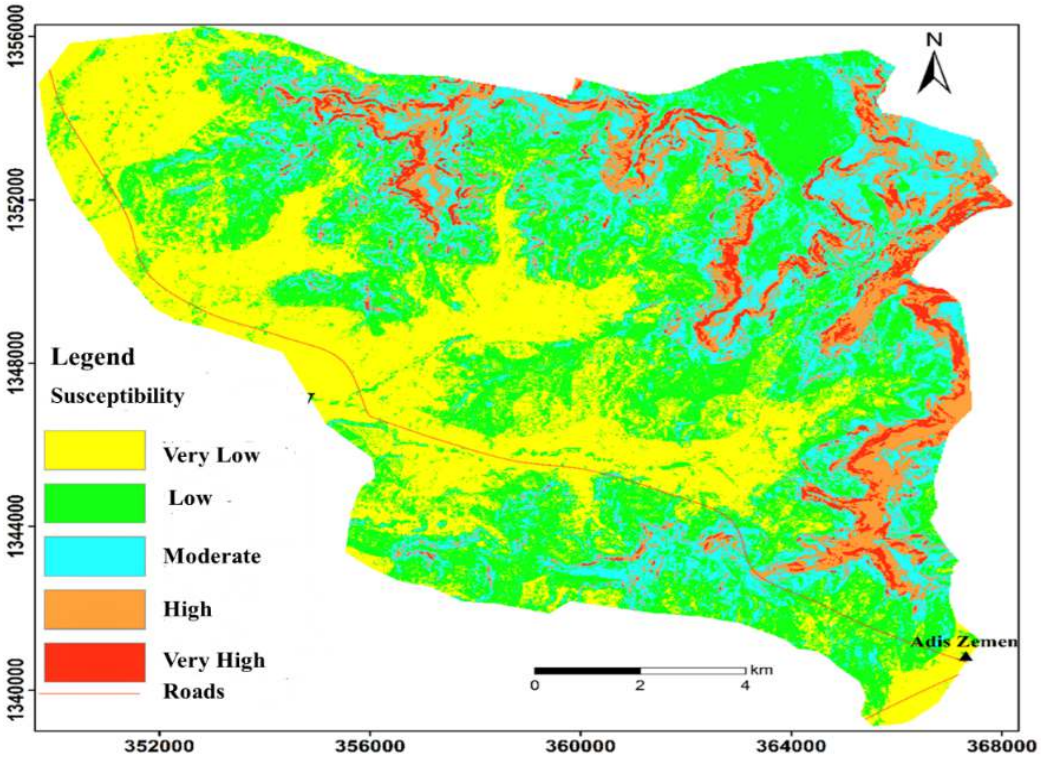

Figure 4. Landslide susceptibility map Enfraz to Addis Zemen using frequency ratio model.

Model validation

The model performance and accuracy were assessed using the AUC of the ROC curve method, which is well-established for model validation (Thanh et al., 2022). The evaluation process included success rate evaluation and prediction rate evaluation. The success rate used to evaluate the model's performance is derived from the training datasets. A high success rate AUC of 92.2%, indicates that the model effectively fits the training data (Thanh et al., 2022; Wubalem et al., 2022; Kohno and Higuchi, 2023; Putriani et al., 2023).

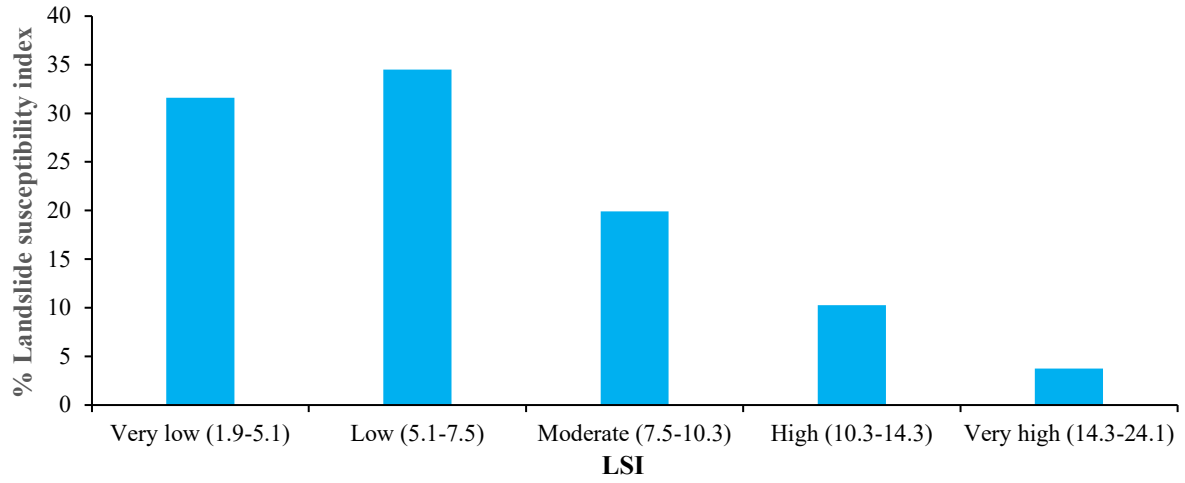

Figure 5. The percentage of landslide susceptibility indexes.

The model was also verified using landslide density and percentages of both training and testing datasets. The results indicate landslide density and percentages increase as LSI increases. This again confirms the model classifies and predicts landslide susceptibility in the region correctly (Figure 7a and b) (Thanh et al., 2022; Menéndez-Duarte et al., 2024).

The model performance and accuracy were assessed using the AUC of the ROC curve method, which is well-established for model validation (Thanh et al., 2022). The evaluation process included success rate evaluation and prediction rate evaluation.

The success rate used to evaluate the model's performance is derived from the training datasets. A high success rate AUC of 92.2%, indicates that the model effectively fits the training data (Thanh et al., 2022; Wubalem et al., 2022; Kohno and Higuchi 2023; Putriani et al., 2023). The prediction rate evaluation used to evaluate the model's accuracy is derived from the validation dataset.

The prediction rate evaluation used to evaluate the model's accuracy is derived from the validation dataset. The prediction rate AUC of 86.03% indicates that the model has a high predictive capacity for new data (Figure 8). This result confirms that the model predicts future landslide occurrences. The comparison between the success and prediction rates emphasizes the importance of model validation. Therefore, model validation using only the success rate or prediction rate is not recommended (Putriani et al., 2023).

Discussion

In this work, the FR model was used to assess the effects of topography, environmental, hydrological, and geological factors on landslide likelihood in the study area. The relationship between factor classes and landslide probability was performed using the FR approach. The results indicate a relationship between factor classes and landslide probability. For example, steeper slopes and higher elevations are strongly associated with high landslide probability. This confirms topography can play a great role in landslide incidence (Figure 9). This result agrees with the findings of (Hang et al., 2021). The slope aspect class of southwest, west, and south-facing slopes are prone to landslides.

This informs the role of slope orientation in landslide probability. As confirmed in the result, these slope orientations are characterized by barren lands, steep gradients, and moderate to high rainfall. Concave and convex slope shapes show a positive relationship with landslide probability. These slope shapes influence water flow, soil deposition, slope gradients, and human activities (Kohno and Higuchi, 2023). In the LULC factor, the woodland class shows a high probability of landslides because of unconsolidated thin soil layers and shallow-rooted vegetation. Field observations show that many trees have shallow roots, which reduces their effectiveness in reinforcing the soil. Moreover, this factor class is situated on a steep slope with shallow soils that are quickly saturated by rainwater. The barren land classes show a relationship with landslide occurrences, likely due to reduced vegetation cover, active soil erosion, and human activities. In contrast, areas covered by bush and forest demonstrate a moderate relationship with landslide probability, indicating that while vegetation provides some degree of protection, it may not be sufficient in highly vulnerable areas when their roots do not cross

the potential failure zones (Wubalem et al., 2022). Distance/proximity to rivers with areas 500 to 1,100 m away from rivers shows a relationship with landslide probability. However, areas closer than 500 m to a river show a low landslide probability. As observed in field observations, areas near the riverbank typically have gentle slopes and solid rocks, playing a great role in this stability problem.

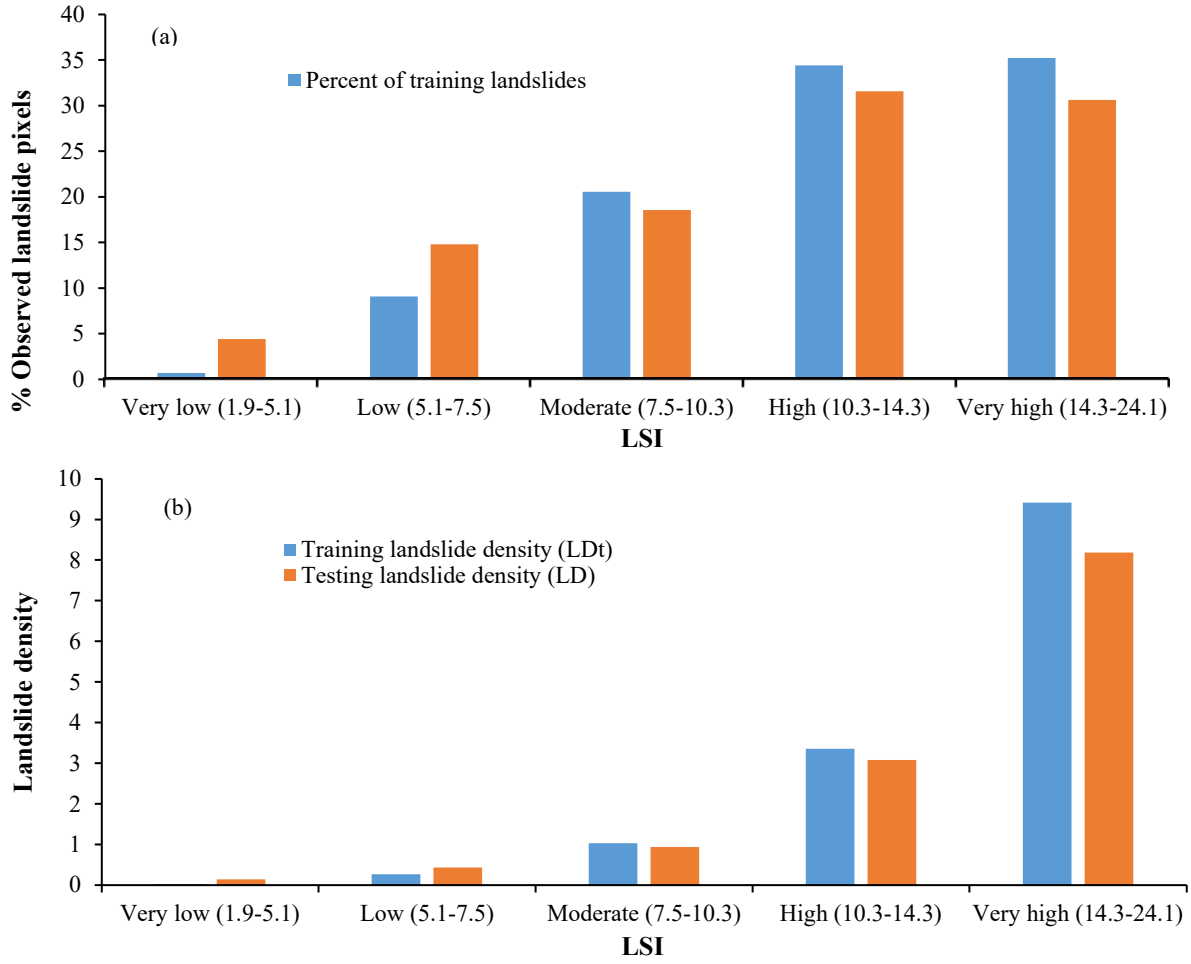

Figure 6. (a) The percent distribution of training and testing landslide areas and (b) The density of training and testing landslides with landslide susceptibility indexes.

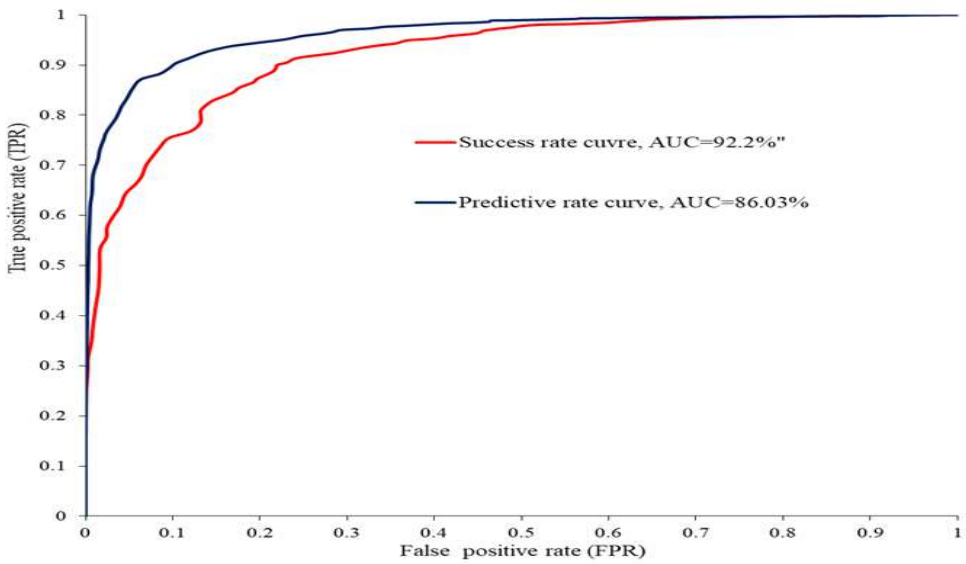

Figure 7. Receiver operating characteristics curve for Enfraz to Addis Zemen area FR model.

Regions with moderate to high precipitation areas show a relationship to landslide probability. Fieldwork and analysis indicate that rainfall impacts landslide risk in areas characterized by scattered woodlands, barren land, unconsolidated thin soil layers, and steep slopes. Lithology controls the size, frequency, and type of landslide (Kohno and Higuchi, 2023). Moderately and highly weathered rocks have a higher relationship of landslide probability, as the weathering weakened the structural integrity of these rocks.

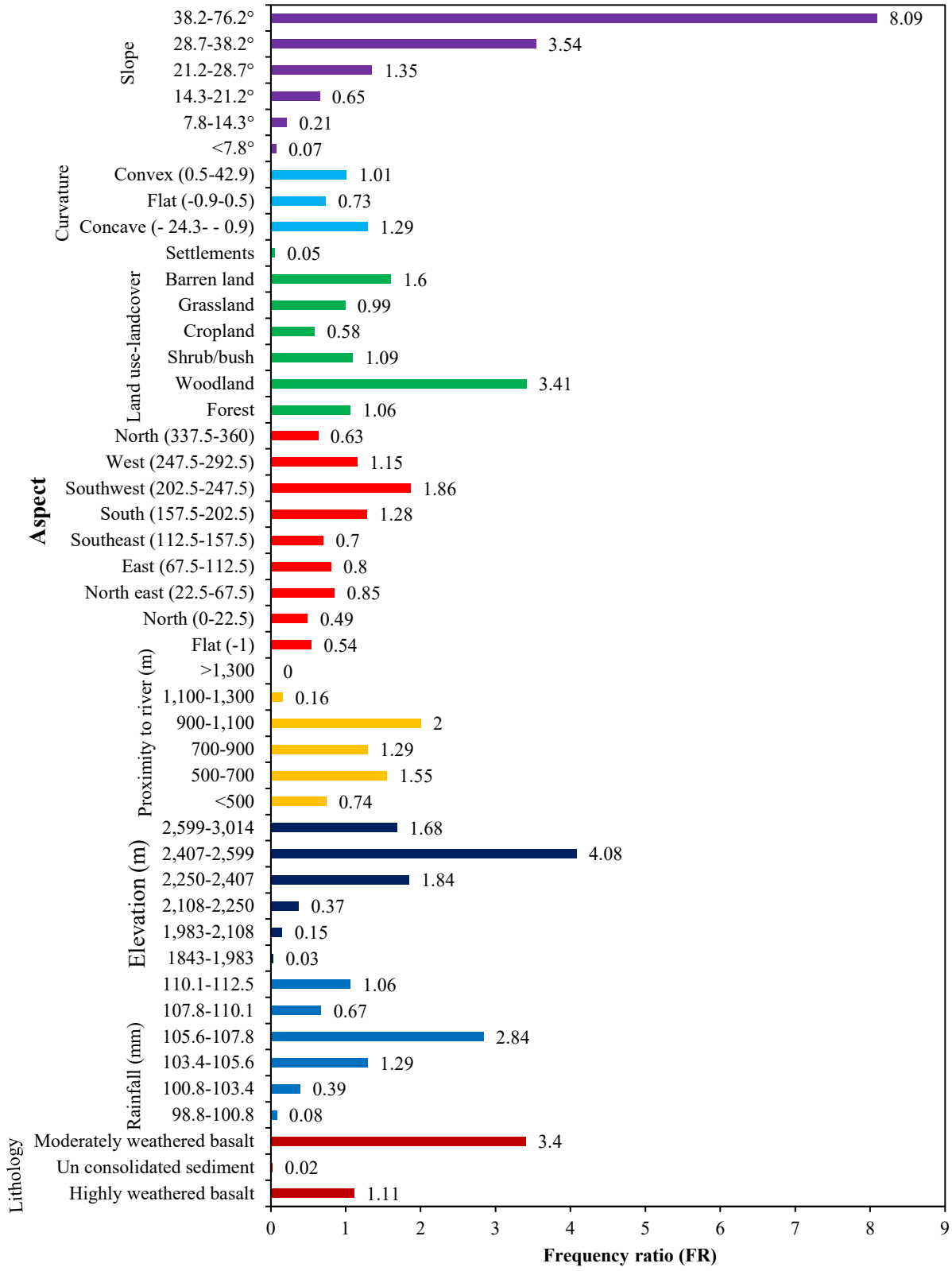

Figure 8. The relationship between different factor classes with landslide probability.

Figure 10 displays the mean value of Frequency Ratio (mFR) for various factors. Slope angle has the highest mFR value, followed by lithology, elevation, LULC, rainfall, and curvature, but aspect and distance/proximity to river show low mFR value. The slope shows its great role in landslide probability. Slope curvature shows a moderate mFR value, indicating its medium effect on landslide probability. The higher mFR of LULC proves that land cover and land use type control landslide probability. Aspect and distance to rivers, both with mFR values below 1, show a minimal effect on landslide probability. Elevation, however, shows a remarkable effect on landslide probability (Yu et al., 2024). Rainfall has a higher mFR value after lithology. It has a great effect on landslide probability in regions with intensive and prolonged rain. Lithology, with its significant impact, highlights how certain rock types and soil conditions increase the likelihood of landslides. The landslide susceptibility map was generated from the sum of weighted parameters under a raster calculator in a GIS environment, classified into five zones of very low, low, moderate, high, and very high susceptibility zones, which is critical for risk assessment and land-use planning (Zhang et al., 2022). The susceptibility zones range from relatively safe regions with flat lands and strong lithology to high susceptibility zones with steep slopes, weak lithology, and low vegetation cover. The central and southwestern parts of the map, dominantly covered by low and very low susceptibility areas, are dominant in a gentle slope class. High and very high susceptibility zones are dominantly distributed in the northeastern and southeastern along the ridge and steep slopes. In these regions, infrastructure development needs careful consideration and possible restrictions.

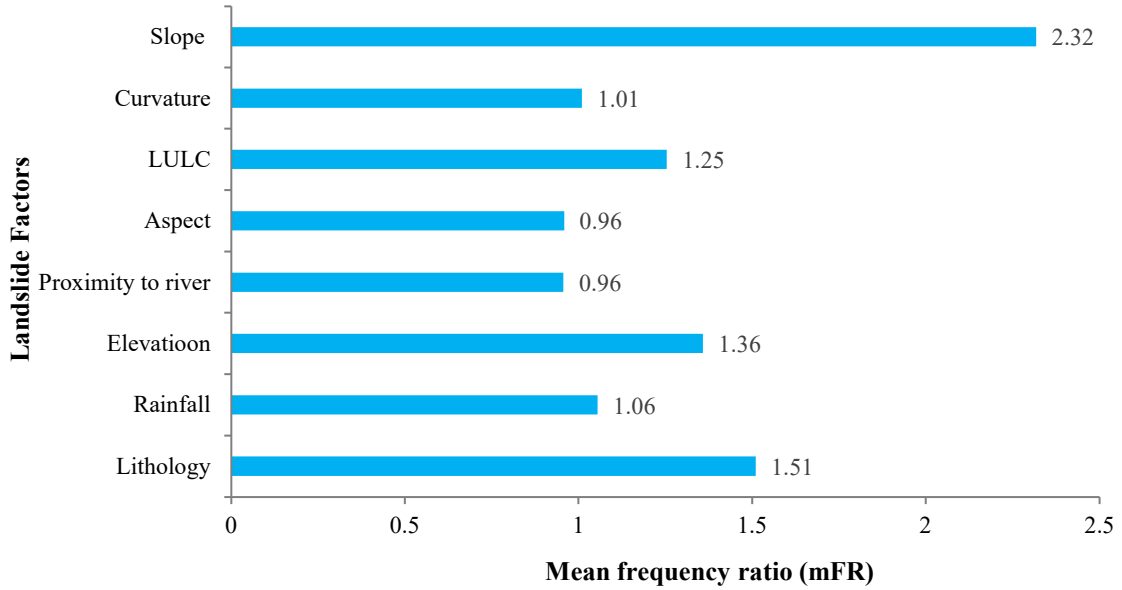

Figure 9. The mean value of FR for each landslide factor.

The quality of the model was validated using the AUC of the ROC curve. The AUC value for success rate is >0.90, and for prediction rate is >0.80. These results indicate the ability of the model to correctly classify the region into landslide-prone and non-prone zones, as well as the model's ability to predict future landslide probability with new landslide datasets (Kohno and Higuchi, 2023). Nachappa et al. (2020) compared the accuracy and performance of the FR method with the AHP method. It was found that the method attained a higher AUC value of 87.8%, which is less than in this study. Author Fang et al. (2021) compared the effectiveness of advanced and traditional machine-learning methods in landslide susceptibility mapping and prediction. They found that the AUC of prediction rates ranges from 77% to 85.8%, slightly lower than the current study AUC prediction rate of 86.03%. The FR model in this study confirms that it is excellent for high-quality landslide susceptibility mapping.

Conclusion

From detailed fieldwork and Google Earth imagery analysis, 134 landslides were identified, including transitional, debris flow, and rock fall types. The analysis revealed that most past landslides are dominantly found on steep slopes, river initiation, close to road cut, moderate to high elevation, scattered woodland-covered areas, barren land, and weathered lithology.

The spatial relationship between landslide factor classes and landslide probability was performed in a GIS environment, and their weights were assigned using the FR model. The result shows the steep slope, weathered lithology, moderate to high elevation, moderate to high precipitation, woodland, barren land, general slope curvature (concave and convex), aspect (south, west, and southwest slope facing), and distance/proximity to the river (500-1,100 m) factor

classes show a high relationship with landslide probability.

The landslide susceptibility map was produced using the FR model, based on the spatial relationship between landslide occurrence and various conditioning and triggering factors. This map was classified into very low, low, moderate, high, and very high susceptibility zones. The very low and low susceptibility zones are dominantly distributed on gentle slope areas, which can be considered relatively safe for infrastructure and agricultural development. However, the moderate, high, and very high susceptibility zones need attention to reduce their negative impact on life, engineering structures, environments, farmlands, villages, and property.

The quality of the model was validated using the AUC of the ROC curve. The result indicates an AUC of success rate of 92.2% and a predictive rate of 86.03%, demonstrating that the FR method classified and predicted the region correctly, implying it is capable of landslide susceptibility modeling. The final FR model of this study can provide valuable information for decision-makers, planners, engineers, and researchers involved in land-use planning, and landslide mitigation strategies. Awareness campaigns could reduce the impact of future landslide events.

This study did not investigate the time series correlation between landslide occurrence and rainfall pattern. Further research shall focus on investigating the effects of climate change on landslide occurrences, focusing on how changes in rainfall patterns and intensity might alter landslide susceptibility in the future.

Acknowledgments

First and foremost, we extend our deepest gratitude to the almighty God for granting us the strength and opportunity to carry out this research. We are also grateful to the University of Gondar for financing this study. We also acknowledge the Ethiopian National Meteorological Agency and the Ethiopian Geological Survey for their invaluable data contributions.

References

Bao, S., Liu, J., Wang, L. and Zhao, X. 2022. Application of transformer models to landslide susceptibility mapping. *Sensors* 22(23), doi:10.3390/s22239104.

Berhane, G., Gebrehiwot, A. and Abay, A. 2023. Landslide susceptibility mapping in the Adwa Volcanic Mountain Plugs, Northern Ethiopia: A comparative analysis of frequency ratio and analytical hierarchy process methods. *Geomatics, Natural Hazards and Risk* 14(1), doi:10.1080/19475705.2023.2281244.

Fang, Z., Wang, Y., Peng, L. and Hong, H. 2021. A comparative study of heterogeneous ensemble-learning techniques for landslide susceptibility mapping. *International Journal of Geographical Information Science* 35(2), doi:10.1080/13658816.2020.1808897.

Gautam, P., Kubota, T. and Aditian, A. 2021. Evaluating underlying causative factors for earthquake-induced landslides and landslide susceptibility mapping in Upper Indrawati Watershed, Nepal. *Geoenvironmental Disasters* 8(1), doi:10.1186/s40677-021-00200-3.

Getachew, N. and Meten, M. 2021. Weights of evidence modeling for landslide susceptibility mapping of Kabi-Gebro locality, Gundomeskel area, Central Ethiopia. *Geoenvironmental Disasters* 8(1), doi:10.1186/s40677-021-00177-z.

Hang, H.T., Hoa, P.D., Tru, V.N. and Phuong, N.V. 2021. Landslide susceptibility mapping along National Highway-6, Hoa Binh Province, Vietnam using Frequency Ratio Model and GIS. *International Journal of GEOMATE* 21(85):84-90, doi:10.21660/2021.85.j2222.

Kohno, M. and Higuchi, Y. 2023. Landslide susceptibility assessment in the Japanese Archipelago based on a landslide distribution map. *ISPRS International Journal of Geo-Information* 12(2), doi:10.3390/ijgi12020037.

Li, B., Liu, K., Wang, M., He, Q., Jiang, Z., Zhu, W. and Qiao, N. 2022. Global dynamic rainfall-induced landslide susceptibility mapping using machine learning. *Remote Sensing* 14(22), doi:10.3390/rs14225795.

Liu, H., Ding, Q., Yang, X., Liu, Q., Deng, M. and Gui, R. 2024. A knowledge-guided approach for landslide susceptibility mapping using convolutional neural network and graph contrastive learning. *Sustainability (Switzerland)* 16(11), doi:10.3390/su16114547.

Martinello, C., Cappadonia, C., Conoscenti, C., Agnesi, V. and Rotigliano, E. 2021. Optimal slope units partitioning in landslide susceptibility mapping. *Journal of Maps* 17(3):152-162, doi:10.1080/17445647.2020.1805807.

Menéndez-Duarte, R., Marquínez, J., Vázquez-Tarrío, D. and Fernández, F.J. 2024. Shallow landslide susceptibility map at a regional scale (Asturias, NW Spain). A heuristic-driven approach. *Journal of Maps* 20(1), doi:10.1080/17445647.2024.2375094.

Mersha, T. and Meten, M. 2020. GIS-based landslide susceptibility mapping and assessment using bivariate statistical methods in Simada area, northwestern Ethiopia. *Geoenvironmental Disasters* 7(1), doi:10.1186/s40677-020-00155-x.

Mulugeta, T., Shano, L. and Jothimani, M. 2024. Landslide susceptibility modeling in the Kulfo river catchment, Rift Valley, Ethiopia: An integrated geospatial and statistical analysis. *Quaternary Science Advances* 14, doi:10.1016/j.qsa.2024.100191.

Nachappa, T., Kienberger, S., Meena, S.R., Hölbling, D. and Blaschke, T. 2020. Comparison and validation of per-pixel and object-based approaches for landslide susceptibility mapping. *Geomatics, Natural Hazards and Risk* 11(1), doi:10.1080/19475705.2020.1736190.

Putriani, E., Wu, Y.M., Chen, C.W., Ismulhadi, A. and Fadli, D.I. 2023. Development of landslide susceptibility mapping with a multi-variance statistical method approach in Kepahiang, Indonesia. *Terrestrial, Atmospheric and Oceanic Sciences* 34(1), doi:10.1007/s44195-023-00050-6.

Roccati, A., Paliaga, G., Luino, F., Faccini, F. and Turconi, L. 2021. GIS-based landslide susceptibility mapping for land use planning and risk assessment. *Land* 10(2):1-28, doi:10.3390/land10020162.

Shano, L., Raghuvanshi, T.K. and Meten, M. 2020. Landslide susceptibility evaluation and hazard zonation techniques – a review. *Geoenvironmental Disasters* 7(1), doi:10.1186/s40677-020-00152-0.

Thanh, L.N., Fang, Y.M., Chou, T.Y., Hoang, T.V., Nguyen, Q.D., Lee, C.Y., Wang, C.L., Yin, H.Y. and Lin, Y.C.

2022. Using landslide statistical index technique for landslide susceptibility mapping: Case study: Ban Khoang Commune, Lao Cai Province, Vietnam. *Water (Switzerland)* 14(18), doi:10.3390/w14182814.

Wubalem, A. 2021. Landslide susceptibility mapping using statistical methods in Uatzau catchment area, northwestern Ethiopia. *Geoenvironmental Disasters* 8(1), doi:10.1186/s40677-020-00170-y.

Wubalem, A. and Meten, M. 2020. Landslide susceptibility mapping using information value and logistic regression models in Goncha Siso Eneses area, northwestern Ethiopia. *SN Applied Sciences* 2(5), doi:10.1007/s42452-020-2563-0.

Wubalem, A., Getahun, B., Hailemariam, Y., Mesele, A., Tesfaw, G., Dawit, Z. and Goshe, E. 2022. Landslide susceptibility modeling using the Index of Entropy and Frequency Ratio Method from Nefas-Mewcha to Weldiya Road Corridor, Northwestern Ethiopia. *Geotechnical and Geological Engineering* 40(10):5249-5278, doi:10.1007/s10706-022-02214-6.

Xiao, T., Yu, L., Tian, W., Zhou, C. and Wang, L. 2021. Reducing local correlations among causal factor classifications as a strategy to improve landslide susceptibility mapping. *Frontiers in Earth Science* 9, doi:10.3389/feart.2021.781674.

Yu, L., Wang, Y. and Pradhan, B. 2024. Enhancing landslide susceptibility mapping incorporating landslide typology via stacking ensemble machine learning in Three Gorges Reservoir, China. *Geoscience Frontiers* 15(4):101802, doi:10.1016/j.gsf.2024.101802.

Zhang, J., Gao, B., Huang, H., Chen, L., Li, Y. and Yang, D. 2022. SBAS-InSAR-based landslide susceptibility mapping along the North Lancang River, Tibetan Plateau. *Frontiers in Earth Science* 10, doi:10.3389/feart.2022.901889.

Zhu, Z., Yuan, X., Gan, S., Zhang, J. and Zhang, X. 2023. A research on a new mapping method for landslide susceptibility based on SBAS-InSAR technology. *Egyptian Journal of Remote Sensing and Space Science* 26(4):1046-1056, doi:10.1016/j.ejrs.2023.11.009.